Available online at www.sciencedirect.com
SCIENCE DIRECT®
Journal of Nuclear Materials 351 (2006) 209–215
journal of nuclear materials
www.elsevier.com/locate/jnucmat

Coincidence Doppler broadening spectroscopy in Fe, Fe–C and Fe–Cu after neutron irradiation

K. Verheyen, M. Jardin, A. Almazouzi *

SCK-CEN, Reactor Materials Research Department, Boeretang 200, B-2400 Mol, Belgium

Abstract

In the framework of the European project PERFECT, dealing with the modelling of irradiated material behaviour, well controlled irradiations have been performed at 300 °C for doses ranging from 0.025 to 0.2 dpa. At this stage, four model-alloys (Fe, Fe–C, Fe–0.1 wt%Cu, Fe–0.3 wt%Cu) have been investigated by Coincidence Doppler Broadening of positron annihilation radiation (CDBAR), a well established tool for studying defects in materials. The results demonstrate the effect of Cu on the matrix damage accumulation under neutron irradiation.

1. Introduction

On the long term, the mechanical properties of pressure vessel steels are known to be modified by neutron irradiation. The problem is studied in the PERFECT project which aims at the modelling of irradiation effects in structural materials [1]. Any modelling effort has to interact with the experimental evidence. If a model does not predict what experiments show, then the model is questionable. However, in the case of multiscale simulation the situation is complicated by the fact that most numerical techniques belonging to this framework have been developed essentially to study phenomena (displacement cascades, dynamics of defect formation, migration, interaction,...) that cannot be directly observed by experimental means. Therefore, the experimental validation of a multiscale model becomes a difficult task, that demands in general the use of advanced experimental techniques, capable of accurately probing the materials at very small scales.

The objective of the experimental validation program of the PERFECT project, is essentially twofold:

- Collect an experimental database to gain deeper insight into the causes of vessel steel embrittlement under irradiation, by analysing not only steels but also model alloys (separation of effects), with post-irradiation characterisations covering the nano-, micro- and mesostructure, up to the macroscopic properties of the irradiated materials.

* Corresponding author. Tel.: +32 14 333096; fax: +32 14 321216.
E-mail address: aalmazou@sckcen.be (A. Almazouzi).

0022-3115/$ - see front matter © 2006 Elsevier B.V. All rights reserved.
doi:10.1016/j.jnucmat.2006.02.011

- Use the data as a reference for the improvement and optimisation of the numerical simulation tools that are being developed in the framework of the project.

The changes in mechanical properties are found to correlate with the formation of various kinds of defects (see e.g. [2–5]). Worldwide, two basic mechanisms are identified to be responsible of the hardening of the Western RPV-steels, namely:

(1) Matrix damage due to radiation induced production of point defect clusters (dislocation loops, nano-voids). It had been established that this effect produces a hardening that increases continuously with irradiation dose in steels [5].
(2) Irradiation enhanced precipitation of Cu-rich nano-clusters. The solubility limit of Cu in Fe at 300 °C is very low. Depending on the literature source, it is quoted to be 0.0002 wt% [6] or 0.05 wt% [7]. In all cases Cu is in excess in the investigated model alloys and will precipitate.

These two effects have been extensively studied by various methods such as high resolution transmission electron microscope (TEM) [8,9], atom probe field ion microscope (APFIM) [10,11], small angle neutron scattering [12] and recently positron annihilation [13,14]. Unfortunately, there are very few studies where all these complementary techniques were used to characterise the same material before and after irradiation at several doses, temperatures and fluxes. Within the PERFECT project, several laboratories have joined their effort to perform such type of study. This paper is reporting on first results obtained within this framework. Its aim is to discuss the interplay between the two mechanisms cited above. In fact, one of the open questions is regarding the amount of vacancies needed to form Cu-nano clusters and the role played by Cu-atoms to trap the irradiation produced vacancies. Several approaches have been used to get a clear answer especially using computer simulation modeling techniques. Thus, using computer simulations based on molecular dynamic method, Osetsky and Serra [15] have found that about 2–6% vacancies are needed to stabilise Cu-precipitates. These authors showed that the precipitates act as trap for the vacancies. This high vacancy concentration arises from the misfit of the Cu-precipitates and from the fact that breaking Fe–Fe or Fe–Cu bonds requires more energy than breaking Cu–Cu bonds. Any cluster of copper atoms that forms would be under compressive stress, which will be reduced by the presence of vacancies mixed with the copper atoms. However, the exact concentration and distribution of vacancies within the precipitates remain undetermined.

Coincidence Doppler Broadening (CDB) of positron annihilation radiation is a powerful technique. By measuring the momentum distribution of the core electrons specific to each element, it is able to identify the chemical elements around the positron annihilation sites and to give at least a qualitative idea on the correlation between vacancies and Cu-atoms. In this paper we will report only the results we obtained by CDB analysis of Fe and Fe–Cu model alloys after neutron irradiation to four different doses. At the time of this conference, lifetime measurements were still in progress and will be reported elsewhere. Our intention is to contribute to the discussion about the exact concentration and distribution of vacancies within the precipitates, by exploring various alternatives.

2. Experiment

2.1. Material

The model alloys with the composition listed in Table 1, were prepared using argon-arc melting and zone refinement methods. The resulted ingots were then cold worked after austenisation tempering. To release the stresses and to get a well recrystalised material a final heat treatment at 1075 K for 1 h followed by a water quench was performed. The average grain size and dislocation density obtained for each of the investigated alloys are also listed in Table 1.

Table 1
Nominal composition, average grain size and dislocation density of the investigated alloys

Material	Nom. Comp. (wt%)	Av. grain size (μm)	Disloc. dens. ($10^{13}/m^2$)
Pure Fe	<30 ppm C	250	7 ± 2
Fe–C	>30 ppm C	350	9 ± 2
Fe–0.1%Cu	0.1 Cu (<30 ppm C)	125	9 ± 2
Fe–0.3%Cu	0.3 Cu (<30 ppm C)	177	9 ± 2

3. Irradiation

The prepared specimens were irradiated in the Callisto rig (IPS2) in the Belgian Reactor (BR2), where the irradiation temperature and pressure were maintained at, respectively, 300 °C and 150 bar. A detailed description of the irradiation characteristics will be published elsewhere [16]. The neutron spectra corresponding to each position occupied by the specimens in the BR2 reactor (midplane and top level), have been calculated using the well know code MCNP. As a first approximation, the spectrum was assumed to be constant in the whole volume containing all capsules of a certain group. Table 2 summarizes the data of flux and fluence. The investigated materials were then irradiated using a fast flux of about 9×10^{13} n/cm^2/s, a value that is at least 100 times higher than in a commercial reactor.

3.1. CDBAR-technique

Recently, at SCK-CEN a new CDBAR-setup has been installed to measure highly radioactive samples. This setup has been described with ample details by Verheyen et al. [17]. The energies of annihilating γ-ray pairs in coincidence (denoted by E_1 and E_2) were simultaneously recorded by two detectors located at an angle of 180° relative to each other. The difference in energies of the two γ-rays, $\Delta E = E_1 - E_2$, is cp_L, and the sum energy $E_T = E_1 + E_2$ is equal to the total energy of the electron–positron pair prior to annihilation, i.e., $2m_0c^2 - E_B$ (neglecting the thermal energies and chemical potentials), where p_L is the longitudinal component of the positron–electron momentum along the direction of the γ-ray emission, c is the speed of light, m_0 is the electron rest mass, and E_B is the electron binding energy. The selection of coincidence events that fulfil the condition $2\,m_0c^2 - 2.4$ keV $< E_T < 2m_0c^2 + 2.4$ keV, results in a significant improvement in the peak to background ratio by three orders of magnitude over conventional one-detector measurements. This enables to observe positron annihilation with element-specific high-momentum core electrons. The overall energy resolution was ≈1.07 keV full width at half maximum (FWHM), which corresponds to the momentum resolution of $\approx 4.2 \times 10^{-3}mc$ (FWHM). All measurements were performed at room temperature using a ^{22}Na positron source of 2MBq strength. More than 1×10^8 counts were accumulated during 48–72 h for each measurement [18].

The analysis of the results has been made using CDB-ratio curves, obtained by normalizing the momentum distribution to the one of unirradiated defect-free pure Fe. The ratio curves emphasize the difference between different elements in the sample. To get a better insight in the obtained spectra, *S*- and *W*-parameters were extracted from each spectrum. The *S*- and *W*-parameters are defined as the ratio of low-momentum ($|cp_L| < 2.5 \times 10^{-3}mc$) and high-momentum ($15 \times 10^{-3}mc < |cp_L| < 25 \times 10^{-3}mc$) regions in the CDB-spectrum to the total region, respectively.

Prior to measurement, the specimens have been chemically etched to minimize the effect of the surface (cold work, contamination or oxidation during irradiation).

4. Results

4.1. Hardening of the material

Fig. 1 shows the variation in yield strength with neutron dose for all four materials investigated. It can be seen that the hardening of all materials has reached the plateau in the typical $\Delta\sigma_y$-to-dose curve. The plateau level is found to depend on the material chemistry such as the addition of Cu induces much more hardening even in model alloys. The yield strength increase depends on the initial Cu-content and already at low dose it rises to reach a plateau value that remains unchanged by subsequent

Table 2
Determined flux and fluence of the materials after irradiation

Group	Flux (10^{13} n/cm^2/s)		Fluence (10^{19} n/cm^2)		Dose (dpa)
	n-thermal	$E_n > 1$ MeV	*n*-thermal	$E_n > 1$ MeV	
1	9.58 ± 0.52	9.5 ± 0.5	12.49 ± 1.05	13.06 ± 1.06	0.19
2	9.54 ± 0.54	8.6 ± 0.5	6.9 ± 0.5	6.93 ±0.52	0.1
3	9.36 ± 0.52	9.0 ± 0.7	1.5 ± 0.7	1.75 ± 0.14	0.026
4	9.32 ± 0.55	9.5 ± 0.5	3.0 ± 0.5	3.46 ± 0.28	0.051

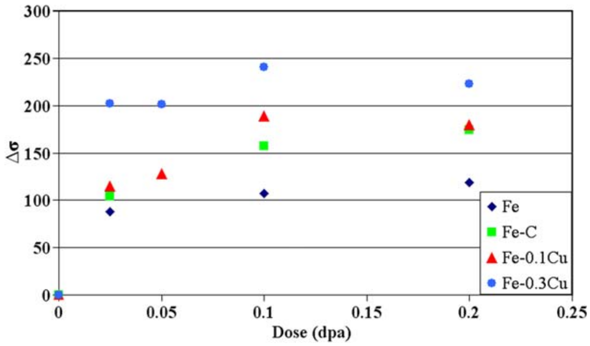

Fig. 1. Increase of yield stress with irradiation dose.

irradiation. It suggests that the additional radiation damage does not affect the yield point of any of the investigated materials in spite of their different chemical composition. In the following, we will be using the CDB results to try to explain these observations.

4.2. CDBAR-results

Figs. 2 and 3 show the CDB ratio-curves, i.e. the momentum distribution normalized to that of defect-free pure Fe, of all irradiated specimens and pure unirradiated Cu. For a better visualization, the spectra were smoothed using a 'running average' method. In each case it has been verified that the used smoothing procedure does not affect the obtained results. The ratio-curves for the irradiated Fe and Fe–C samples (Figs. 2(a) and (b)) show an increase in the low and a decrease in the high momentum region. This is due to the presence of irradiation induced vacancy-type defects in which the positrons are preferentially trapped.

In Figs. 3(a) and (b) the CDB ratio-curves for the Fe–0.1Cu and Fe–0.3Cu samples and also the characteristic features of the CDB signal of pure Cu are reported. The latter shows a small valley around $6 \times 10^{-3} mc$ and a broad peak at $25 \times 10^{-3} mc$. The ratio-curves for the Fe–Cu samples show an increase in the low momentum region and a small broad peak at around $25 \times 10^{-3} mc$. The increase in the low momentum region indicates the presence of vacancy-type defects, while the curves in the high momentum region clearly reveal the presence of Cu atom clusters that may contain vacancies. The latter effect is more pronounced in the signals obtained from Fe–0.3Cu samples than from those of Fe–0.1Cu samples.

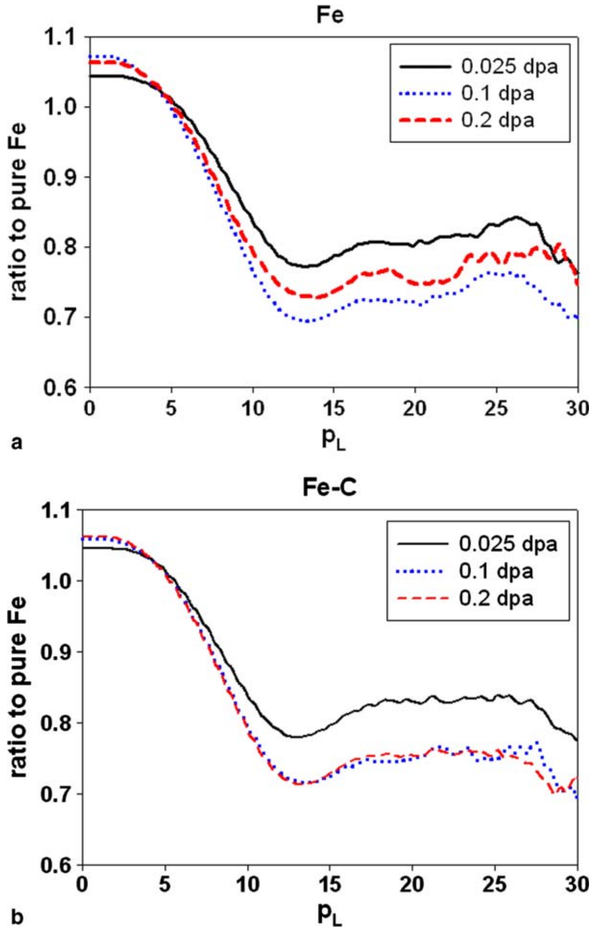

Fig. 2. (a) Ratio-curves of Fe and (b) ratio-curves of Fe–C.

Fig. 4 shows the evolution of the S- and W-parameters with the irradiation dose. The point described as 'pure Fe' represents the defect free iron. Due to its high activity some difficulties occurred when measuring the pure Fe irradiated to 0.1 dpa, which makes its values of the S- and W-parameter a bit uncertain. However the S- and W-parameters for Fe follow the same trend as the Fe–C samples. The dotted lines in Fig. 4(a) and (b) have to be considered as 'guiding eyelines'. For all materials the S-parameter (Fig. 4(a)) increases markedly after neutron irradiation, while the W-parameter decreases (Fig. 4(b)).

5. Discussion

Fig. 4(a) and (b) demonstrates that the behaviour of Fe–Cu binary alloys is quite different from this of Fe or Fe–C. For Fe and Fe–C, the S-parameter increases already after 0.02 dpa irradiation

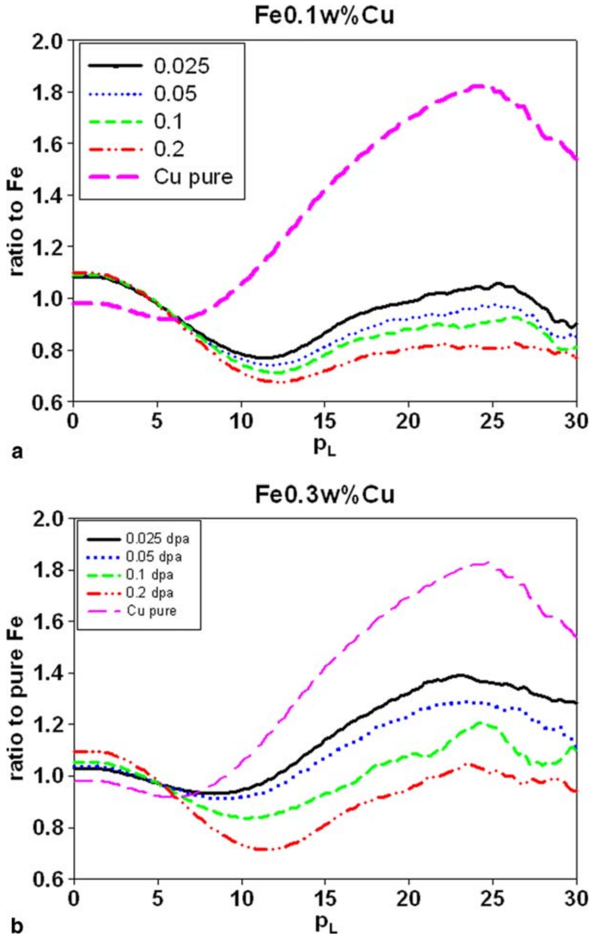

Fig. 3. (a) Ratio-curves of Fe–0.1Cu and (b) ratio-curves of Fe–0.3Cu.

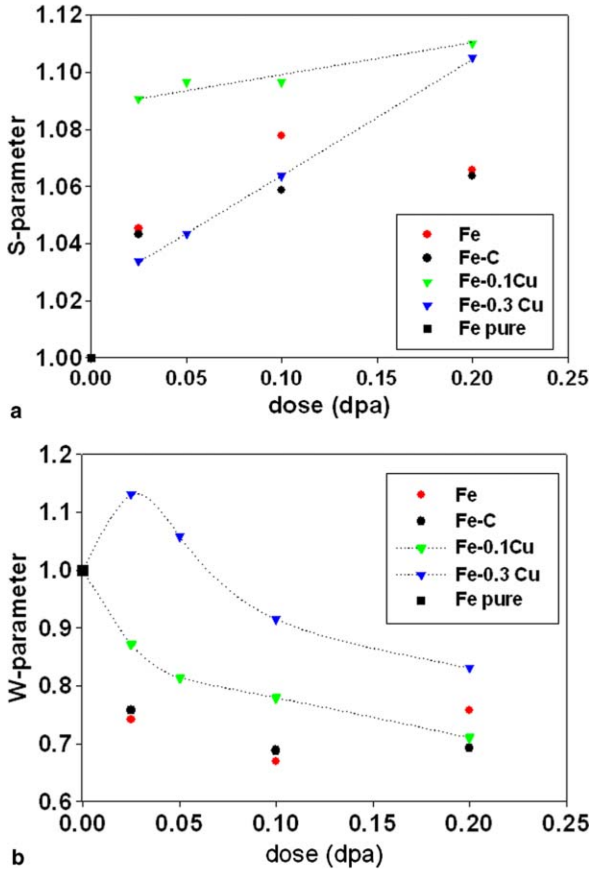

Fig. 4. (a) *S*-parameter vs. irradiation dose and (b) *W*-parameter vs. irradiation dose.

indicating an increase of either the size and/or the density of the vacancy-type defects that trap positrons. This result is in agreement with the first results of the lifetime measurements that are being performed on the same materials [19]. At higher doses the *S*-parameter saturates. Three reasons are considered to be at the origin for the saturation at high doses:

(1) the defect density does not increase substantially with irradiation dose;
(2) the defect density exceeds an upper limit above which the sensitivity for the positron annihilation diminishes;
(3) the defects are growing in size which results in a decreasing density.

Obviously, it is rather difficult to decide which of these mechanisms could be the dominant one, although our first LT results [19] which are in qualitative agreement with those obtained by Eldrup and Singh [20], suggest that mechanism (1) would be most likely in Fe and Fe–C materials. The *S*-parameter for the Fe–Cu alloys increases linearly with the irradiation dose. In contrast to the Fe and Fe–C samples there is no saturation at high doses. This apparent contradiction could be explained by the fact that Cu is playing the role of vacancy clustering site. Therefore, the density of the defects will keep increasing but not necessary their size. The *S*-parameter for the Fe–0.1Cu samples is higher than for Fe and Fe–C indicating the presence of more efficient trapping sites in this material. Hence, if a small amount of Cu is added to Fe, the material will contain a higher density of vacancy clusters and/or bigger vacancy-clusters or voids after irradiation at the same dose. This confirms that Cu-clusters act as a trap for vacancies [15]. The first lifetime results indeed show a longer lifetime in the Fe–0.1Cu samples compared to the Fe–C samples [19,21].

The *S*-parameter for the Fe–0.3Cu is smaller at the lowest dose (0.025 dpa) compared to the sample with lower Cu-content (Fe–0.1Cu), but it evolves to about the same value at the highest dose. This observation is quite important as it illustrates that the microscopic defects introduced by irradiation would not necessary influence the macroscopic hardening of the material. In order to illucidate this observation, it is important to remind that Cu has also a high affinity to positrons and therefore both vacancy and Cu clusters are acting as competitive trapping sites for the incoming positrons. The latter phenomenon is treated in the literature with the so-called two defect trapping model [22] which we will not discuss in detail here. Nevertheless in the following we will use the fact that qualitatively vacancies and Cu-atoms are very big competitors towards positrons and there is no clear theory that would help distinguishing their specific contribution. At this point, it is therefore obvious that the discussion of the *S*-parameter behaviour in comparison with the materials hardening cannot be made without discussing the *W*-parameter first. Before going on with the discussion, it is necessary to make clear some definitions. In the following, Cu-peak is defined as the difference between the lowest (around $12 \times 10^{-3} mc$) and the highest (around $25 \times 10^{-3} mc$) values of the ratio curves to pure Fe. Furthermore, the Cu-height is defined as the value of the ratio curves to pure Fe at $25 \times 10^{-3} mc$. It has been already demonstrated using thermal ageing experiments of super-saturated Fe–Cu alloys, that both Cu-peak and Cu-height increase monotonically with the size and/or the density of Cu-precipitates [17]. However, as can be seen in Fig. 3(a) and (b), in this case (under neutron irradiation) the Cu-height is decreasing while the Cu-peak stays about constant with increasing dose. The results demonstrate that in fact all excess Cu has precipitated already at low dose and these precipitates will contain more and more vacancies as the irradiation dose increases. Looking at Fig. 4(b) where the dotted lines have to be considered as 'guiding eyelines', one can see that as expected the *W*-parameter has increased steadily after irradiation up to 0.02 dpa and thereafter decreased with dose. In the low Cu alloy the *W*-parameter decreases continuously with dose in contrast to what has been stated by Fujii et al. [23] when analysing low Cu steels irradiated with much lower flux neutrons or electrons. In fact, a close examination of their data show that their measured *W*-parameter is also decreasing with dose.

When comparing the results obtained from mechanical testing with those from CDB, it appears that the hardening increase is mainly due to the initial amount of Cu in Fe and that the vacancy clusters are relatively weak dislocation obstacles independently of the extend of Cu-covering.

6. Conclusions

Model alloys that have been irradiated to four different doses, up to 0.2 dpa, under well controlled conditions are being investigated within the PERFECT project using various experimental techniques. This paper reported on the first results obtained by our newly installed CDBAR-technique. It has demonstrated that in model Fe–Cu alloys Cu plays the role of a nucleation site of vacancy clusters, which grow with the irradiation dose. These clusters were found to be weak obstacles towards dislocation movement.

Acknowledgements

Many thanks to BR2 and the technology teams of SCK-CEN for their effort on performing well controlled irradiation. This project would not have exist without the enthusiasm and effort of S. Jumel and J.C. Van Duysen from EDF. The continuous support and help of our colleagues from the department of Reactor Materials Research at SCK-CEN are kindly acknowledged. This work was partly supported by the European Commission in the framework of the PEREFCT-project under contact number: F16O-CT-2003-508840.

References

[1] Integrated project within the 6th frame work program contract number: F16O-CT-2003-508840. Available from: <www.perfect.net>.
[2] J.T. Buswell, W.J. Phythian, R.J. McElroy, S.J. McElroy, S. Dumbill, P.H.N. Ray, J. Mace, R.N. Sinclair, J. Nucl. Mater. 225 (1995) 196.
[3] E.D. Eason, J.E. Wright, G.R. Odette, NUREG/CR 6551, November 1998.
[4] M. Kirk, EPRI MRP/NRC, Maryland, 30 August 2000.
[5] C.A. English, J.M. Hyde, S.R., in: Proceeding of International Symposium on the Mechanisms of Materials Degradation and Non-Destructive Evaluation in Light Water Reactors, Osaka (Japan), 27–29 May 2002, p. 53;
K. Fukuya, H. Nakata, K. Fujii, Characterization of radiation-induced microstructural changes in reactor vessel steels.

[6] G. Salje, M. Feller-Kniepmeier, J. Appl. Phy. 48 (1977) 1833.
[7] M. Perez, F. Perrard, V. Massardier, X. Kleber, A. Deschamps, H. De Monestrol, P. Pareige, G. Covarel, Philos. Mag. 85 (2005) 2197.
[8] W.J. Phytian, A.J.E. Foreman, C.A. English, J.T. Buswell, M. Hetherington, K. Roberts, S. Pizzini, ASTM STP 1125, 1992, p. 131.
[9] M.L. Jenkins, M.A. Kirk, J. Nucl. Mater. 273 (2000).
[10] M.K. Miller, K.F. Russel, P. Pareige, M.J. Starink, R.C. Thomson, Mater. Sci. Eng. A 250 (1998) 49.
[11] P. Auger, P. Pareige, S. Welzel, J.C. Van Duysen, J. Nucl. Mater. 280 (2000) 331.
[12] J. Boemert, H.W. Viehrig, A. Ulbricht, J. Nucl. Mater 334 (2004) 71.
[13] Y. Nagai, Z. Tang, M. Has egawa, T. Kanai, M. Saneyasu, Phys. Rev. B 63 (2001) 134110.
[14] P. Asoka-Kumar, B.D. Wirth, P.A. Sterne, Philos. Mag. Lett. 82 (2002) 609.
[15] Yu.N. Osetsky, A. Serra, Philos. Mag. A 75 (1997) 1097.
[16] B. Verboomen, SCK-CEN-IR-0013, 2002.
[17] K. Verheyen, M. Jardin, A. Almazouzi, SCK-CEN-BLG-957, 2004.
[18] M. Jardin, K. Verheyen, A. Almazouzi, T. Takeshi, Y. Nagai, SCK-CEN-BLG 983, 2004.
[19] K. Verheyen, M. Jardin, A. Almazouzi, submitted for publication.
[20] M. Eldrup, B.N. Singh, J. Nucl. Mater. 323 (2003) 346.
[21] B.D. Wirth, Thesis Santa Barbara, University of California, 1998.
[22] M.J. Puska, R.M. Nieminen, Rev. Mod. Phys. 66 (1994) 853.
[23] K. Fujii, K. Fukuya, N. Nakata, K. Hono, Y. Nagai, M. Hasegawa, J. Nucl. Mater. 340 (2005) 247.